Current Research in Toxicology 8 (2025) 100207

Contents lists available at ScienceDirect

Current Research in Toxicology

journal homepage: www.journals.elsevier.com/current-research-in-toxicology

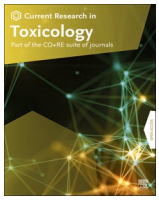

Research Paper

RhoA/ROCK2 signaling pathway regulates Mn-induced alterations in tight junction proteins leading to cognitive dysfunction in mice

Yan Ma [a], Honggang Chen [a], Yuxin Jiang [a], Diya Wang [a], Michael Aschner [c], Wenjing Luo [a,*], Peng Su [a,b,*]

[a] Department of Occupational & Environmental Health and the Ministry of Education Key Lab of Hazard Assessment and Control in Special Operational Environment, School of Public Health, Fourth Military Medical University, Chang Le Xi Road, Xi'an,Shaanxi 710032, China
[b] Department of Occupational and Environmental Health, School of Public Health, Chongqing Medical University, Chongqing 400016, China
[c] Department of Molecular Pharmacology, Albert Einstein College of Medicine, New York, United States of America

ARTICLE INFO

Keywords:
Manganese
Tight Junction
RhoA
Gastrodin

ABSTRACT

Elevated manganese (Mn) exposure has been implicated in a broad spectrum of neurological disorders, including motor dysfunction and cognitive deficits. Previous studies have demonstrated that Mn induces neurotoxicity by disrupting the integrity of the blood–brain barrier (BBB), a critical regulator in maintaining central nervous system homeostasis and a contributing factor in the pathogenesis of numerous neurological disorders. However, the precise molecular mechanisms underlying Mn-induced BBB disruption and its role in facilitating neurotoxicity remain incompletely understood. The primary objectives of this study were to elucidate the mechanisms underlying the relationship between Mn exposure and BBB tight junction proteins (TJPs), and to further investigate potential neuroprotective strategies for mitigating Mn-induced cognitive impairments. In this investigation, we developed Mn exposure models utilizing both murine subjects and cell culture systems to elucidate the mechanisms underlying TJPs involvement and to assess the potential neuroprotective effects of gastrodin (GAS), a bioactive compound extracted from traditional Chinese medicine. Our findings revealed a significant reduction in TJPs expression, both *in vivo* and *in vitro*, in Mn-induced BBB disruption. The overexpression of Occludin (OCLN), a crucial component of TJPs, mitigated Mn-induced BBB damage. GAS administration effectively attenuated Mn-induced disruption of the BBB, enhanced the expression of TJPs, and mitigated Mn-induced cognitive dysfunctions, potentially through the modulation of the RhoA/ROCK2 signaling pathway. This research sought to advance our understanding of the molecular pathways involved in Mn-mediated BBB disruption and to identify novel therapeutic approaches for mitigating the deleterious effects of Mn exposure on cognitive function.

1. Introduction

Manganese (Mn) is an essential trace element crucial for human physiology, required in minute quantities for optimal bodily functions. It plays a vital role in the growth and development of organisms and confers numerous health benefits. Various dietary sources, including nuts, chocolate, tea, and whole grains, serve as significant contributors to Mn intake (Peres et al., 2016). The significance of Mn as a trace element is paramount; while adequate levels are necessary for maintaining optimal physiological functioning, excessive amounts can lead to neurotoxicity (Balachandran et al., 2020). Elevated Mn concentrations in the brain are typically attributed to environmental overexposure, including occupational exposure to high Mn levels or consumption of Mn-contaminated drinking water (Guilarte, 2013; Li et al., 2021b; Roh et al., 2016). Excessive Mn exposure primarily manifests as motor disorders and can significantly impair cognitive function. However, the underlying mechanism of Mn-induced neurotoxicity is not yet fully understood. In this study, we developed Mn exposure models utilizing both murine subjects and cell culture systems to elucidate the detailed mechanisms of Mn neurotoxicity.

The blood–brain barrier (BBB) is a highly dynamic interface between the circulatory system and the brain, serving as a crucial component and

* Corresponding authors at: Department of Occupational and Environmental Health, School of Public Health, Chongqing Medical University, Chongqing 400016, China.
E-mail addresses: luowenj@fmmu.edu.cn (W. Luo), sphm1987@fmmu.edu.cn (P. Su).

https://doi.org/10.1016/j.crtox.2024.100207
Received 29 October 2024; Received in revised form 19 November 2024; Accepted 5 December 2024
Available online 18 December 2024

protective barrier of the central nervous system (CNS). Current evidence suggests that BBB dysfunction is implicated in the pathogenesis of nearly all neurological disorders (Sulzer, 2007). The BBB is composed of pericytes, microvascular endothelial cells, and astrocytes, which collectively regulate and maintain BBB function (Takata et al., 2021; Zhao et al., 2022). Tight junction proteins (TJPs), including Occludin (Ocln), junctional adhesion molecules (JAM), ZO-1 and claudin-1, are integral components of the barrier system, playing a critical role in maintaining its structural and functional integrity (Li et al., 2021a; Zlokovic, 2008). Studies have shown that excessive Mn induced BBB disruption, but the specific effects of excessive Mn exposure on BBB tight junction proteins remain to be elucidated.

Rhizoma Gastrodiae (*G. elata*), a well-documented medicinal herb, is primarily valued for its rhizome, which contains gastrodin (GAS) as its principal bioactive constituent (Tao et al., 2009). GAS exhibits a diverse array of pharmacological properties (Ojemann et al., 2006; Peng et al., 2013), and its broad therapeutic potential in various neurological conditions has garnered considerable attention in the neural scientific field (Li et al., 2019). *In vitro* studies have elucidated GAS's capacity to attenuate oxidative stress and modulate the p38 MAPK/Nrf2 pathway, thereby conferring neuroprotection to dopaminergic neurons (He et al., 2021; Jiang et al., 2014; Zhang et al., 2016). Moreover, GAS has demonstrated efficacy in preserving blood–brain barrier (BBB) integrity by maintaining tight junction proteins and reducing BBB permeability in neurocognitive disorders (Li et al., 2021a). Despite these promising findings, the potential protective effects of GAS against Mn toxicity and its underlying molecular mechanisms remain to be fully elucidated.

The RhoA-ROCK signaling pathway has been implicated in the pathogenesis of several neurological disorders (Iyer et al., 2021; Tonges et al., 2012). Previous research has extensively documented the critical role of the RhoA/ROCK signaling pathway in maintaining the integrity of the blood–brain barrier (BBB). Inhibition of this pathway has been shown to prevent the depolymerization of cytoskeletal actin in brain microvascular endothelial cells (BMECs) and mitigate the downregulation of tight junction proteins (Zamboni et al., 2018). RhoA, a small GTPase belonging to the Ras superfamily, regulates various cellular functions and plays a crucial role in central nervous system development (Schmidt et al., 2022). Given the established role of the RhoA/ROCK pathway in BBB maintenance and its implication in neurodegenerative processes, it is imperative to investigate whether this signaling cascade mediates the alterations in BBB tight junction proteins caused by excessive Mn exposure. In the current research, we found that GAS administration effectively attenuated Mn-induced disruption of the BBB, enhanced the expression of TJPs, and mitigated Mn-induced cognitive dysfunctions, potentially through the modulation of the RhoA/ROCK2 signaling pathway.

2. Materials and methods

2.1. Antibodies and reagents

Gastrodin (GAS) was obtained from Aladdin (Shanghai, China). Abcam supplied ZO-1 (ab221547), Ocln (ab216327), anti-rabbit secondary antibodies (Alexa Fluor 488) (A21206), anti-mouse HRP-linked antibody (7076S), and anti-rabbit HRP-linked antibody (7074S). Sigma-Aldrich (St. Louis, MO, USA) provided Corning® Transwell® cell culture inserts (CLS3470) and FITC-Dextran (46945). HA-1077, a RhoA/ROCK signaling pathway inhibitor, was purchased from Topscience.

2.2. Animals and exposure

Male Cdh5-Cre and female R26-tdTomato mice, aged 6–8 weeks, were procured from Cyagen (Suzhou, China). C57BL/6 male mice aged 6–8 weeks were obtained from the Animal Center of Fourth Military Medical University. All procedures involving animals were performed following the standards of animal care guidelines. Throughout the experiment, mice were maintained at a constant temperature of 24 °C and approximately 45 % humidity with a 12-h light/dark cycle.

The animals used in the experiments were as follows: (i) Cdh5-Cre$^{+/-}$ and Cdh5-Cre$^{-/-}$ mice were obtained by mating the purchased male Cdh5-Cre$^{+/-}$ mice with C57BL6 mice, and the genetic identification information was shown in Supplement Fig. 5A. (ii) Hybridization of male Cdh5-Cre$^{+/-}$ and female R26-tdTomato$^{+/+}$ mice resulted in the generation of R26-tdTomato-Cdh5-Cre offspring expressing red fluorescent protein in endothelial cells, and the identification information of the mice was shown in Supplement Fig. 5B. Mice of 6–8 weeks male were selected for the experiment.

In accordance with the experimental design, pre-treatment was administered to the Control (Con), Gastrodin (GAS), and Manganese plus Gastrodin (Mn + GAS) groups via abdominal subcutaneous injection of GAS (100 mg/kg) or vehicle on days 1, 3, and 5. Preconditioning with GAS (50,100 and 200 mg/kg) could significantly improve the BBB damage induced by cerebral ischemia during perfusion, and the results showed that 100 mg/kg dose was especially significant. A dose of 100 mg/kg was therefore used for pretreatment in our experiments (Li et al., 2019). The GAS solution was prepared by dissolving 0.1 g of the compound in 10 ml of 0.9 % saline. Subsequent to this pre-treatment regimen, Mn was administered following previously established protocols (Wang et al., 2017). The blood samples were collected from the heart for the determination of blood manganese content. The blood samples were perfused with normal saline to remove excess blood. The tissues used for molecular biology experiments were frozen at −80 °C, and the tissues used for immunofluorescence were placed in 4 % paraformaldehyde.

2.3. Contextual fear conditioning

Cognitive ability assessment was conducted utilizing the Mouse Fear Conditioning System (Med Associates, USA). The experimental protocol encompassed a three-day procedure. On the initial day of the conditioning phase, auditory stimulation (2.3 kHz; 70 dB) was administered at 10-second intervals for a duration of 5 min. The subsequent day involved the presentation of an acoustic stimulus (2.3 kHz; 70 dB) for 30 s, culminating in a synchronous 2-second electrical shock (0.75 mA). This sequence was iterated thrice, with the subjects being removed from the conditioning chambers 30 s post-final shock administration (Viellard et al., 2016). On the third day, auditory stimulation (2.3 kHz; 70 dB) was delivered once every 10 s. This protocol was executed daily for three consecutive days under standardized conditions. Memory function under the influence of the conditioned stimulus was quantified by measuring the percentage of freezing behavior exhibited over a 5-minute observation period.

2.4. Novel object recognition test

Mice were placed in a square arena measuring 400 mm × 400 mm. During the training phase, two identical cylindrical objects were positioned at opposite diagonal corners of the arena's base. The mice were allowed to freely explore these objects for a 5-minute period. Following this familiarization phase, one of the original objects was replaced with a novel object of a different shape for the test phase. The cognitive ability of the mice was quantified using the discrimination index (DI), calculated as follows: DI = [(Time spent exploring novel object − Time spent exploring familiar object)/(Total exploration time for both objects)] × 100 %.

2.5. Blood manganese (Mn) concentration analysis

Following the completion of the animal behavior study, a blood sample (0.1 mL) was extracted from the heart under sodium pentobarbital anesthesia. Mn concentration was determined using hydride generation atomic fluorescence spectrometry, in accordance with national

standard methods.

2.6. Permeability assays in vitro and in vivo

In *vivo*, experimental animals received an intravenous injection of 2 % fluorescein sodium (2 mL/kg) via the tail vein. After approximately 30 min, anesthesia was induced by intraperitoneal injection of 10 % sodium pentobarbital (3 mL/kg), followed by perfusion with normal saline. Subsequently, various brain regions were harvested from the fluorescein-injected mice, blotted with filter paper, and subjected to extraction using 30 % trichloroacetic acid. Optical density (OD) measurements were performed at 440 nm excitation and 525 nm emission wavelengths(Li et al., 2021a).

In *vitro*, BEnd.3 cells were seeded in 6.5-mm Transwell® plates at the cell density of 1 × 10^4 cells per well with 0.4 μm Pore Polycarbonate Membrane Inserts (Corning, NY). Following convergence, Mn (100 μM) was added for 24 h. The next test was of the permeability of FITC-dextran in various molecular weights. The transepithelial permeability was estimated with 20 μg/mL FITC-dextran (molecular weight of 4 kDa and 70 kDa) (Kim et al., 2020) in phosphate buffered saline (PBS). Subsequently, the integrity of the junction was assessed and the OD values were obtained and represented under 490 excitation and 520 nm emission wavelengths.

2.7. Cell culture conditions

The bEnd.3 cell line (immortalized mouse brain endothelial cells) was utilized for *in vitro* experiments. Cells were cultured in Dulbecco's Modified Eagle Medium (DMEM) supplemented with 10 % fetal bovine serum (FBS), 100 units/mL penicillin, and 100 μg/mL streptomycin. The bEnd.3 cells were maintained in an incubator at 37 °C with 5 % CO_2 and 95 % air.

2.8. Cell viability assessment

BEnd.3 cells were seeded onto 96-well plates and exposed to varying concentrations of Mn for durations of 6, 12, 24, or 48 h. Subsequently, 0.5 mg/mL of 3-(4,5-dimethylthiazol-2-yl)-2,5-diphenyltetrazolium bromide (MTT) was added and incubated for 4 h. Absorbance values were measured at a wavelength of 570 nm to assess cell viability.

2.9. RNA extraction and RT-qPCR

Total RNA was extracted from bEnd.3 cells and mouse brain tissue using TRIzol reagent (Takara, Japan) according to the manufacturer's instructions. Detailed methodologies can be found in the Supplementary Material and Methods section. The primer sequences utilized in the experiments are presented in Table 1. β-actin was selected as the reference gene for normalization.

2.10. Immunostaining

The experimental protocol involved seeding 5000 cells per well onto small circular slides within a 6-well plate. Upon reaching confluence, the cells were subjected to a 24-hour Mn treatment. Post-treatment, the cells were fixed in ice-cold methanol and subsequently permeabilized with a buffer containing 0.25 % Triton X-100 in PBS for 30 min. Each slide was then blocked with 5 % BSA for an additional 30 min. Primary antibodies diluted in 5 % BSA were applied for overnight incubation at 4 °C. The following day, fluorescent rabbit/mouse secondary antibodies diluted in PBS were used for incubation at room temperature for 2 h. Finally, the slides were mounted using a DAPI-containing mounting solution.

Table 1
Primer Sequence.

Number	Gene	Sequence(3′-5′)
1	ZO-1-F	TGAGCCGGTGTCTGATAATG
2	ZO-1-R	TTCTGTTCGCTCTCCTCTCC
3	Claudins-1-F	GTAATTGGCATCCCCTTGCT
4	Claudins-1-R	ATCATCTTCCAGGCACCTCA
5	Claudins-2-F	TTTGGTAGCCGGAGAGATTG
6	Claudins-2-R	GGAGAGCTCCTAGTGGCAAG
7	Occludin-F	TCCAGGACATTCATCGCTTC
8	Occludin-R	GATCGTGGCAATAAACACCA

2.11. Western blot

Subsequent to rinsing the cells or tissues with PBS, lysis was performed using a homogenizer in RAPI lysates containing a 1 % mixture of protease hydrolase and phosphatase inhibitors. Protein samples were lysed in loading buffer for 10 min at 100 °C. Equal amounts of protein samples (30 μg/lane) were resolved by Tris–HCl, the membranes were then blocked with BSA. Primary antibodies for ZO-1, Ocln, β-actin (hour 4 °C incubation) were added and then followed with HRP-conjugated secondary antibodies. Finally, the protein expression was normalized with the loading control, and quantitation was performed using ImageJ software.

2.12. Statistics analysis

Means ± SEM were determined. Two-group comparisons were performed using Student's *t*-test and multiple-group comparisons were performed using two-way ANOVA followed by Tukey's multiple comparison test. Statistical analyses were conducted using GraphPad Prism 8.0 software. Sample size $N \geq 3$ for each set of data and a significance level of $p < 0.05$ was used.

3. Result

3.1. Mn exposure exposure impairs cognitive function and compromises blood–brain barrier integrity in mice

This study employed Cdh5-Cre mice to investigate vascular morphology and integrity. These mice were crossed with R26-tdTomato reporter mice to generate offspring expressing red fluorescent protein in endothelial cells (Fig. 1A). Specifically, R26-tdTomato-Cdh5-Cre$^{-/+}$ and R26-tdTomato-Cdh5-Cre$^{-/-}$ mice were obtained, with R26-tdTomato-Cdh5-Cre negative mice serving as controls (Con).

A subacute manganese (Mn) exposure model was established as illustrated in Fig. 1A. Mn levels in blood were quantified using atomic fluorescence spectrophotometry (Fig. 1B). The Mn-exposed group exhibited a ~30-fold increase in blood Mn levels compared to the control group. Further analysis revealed elevated Mn levels in both cortical and hippocampal regions two weeks post-exposure (Fig. 1C and Fig. S1A).

To assess cognitive function following Mn exposure, we conducted novel object recognition and fear conditioning tests. The novel object recognition test revealed a significant decline in the mice's ability to discriminate new objects (Fig. 1E, G, and H). The fear conditioning test, which provides insights into short-term memory under conditioned stimuli, showed no significant difference in freezing time percentage between Mn-exposed and control groups on the first day of conditioning. However, on the second day (acoustic and electrical co-stimulation) and the third day (acoustic stimulus alone), the Mn-exposed group exhibited a significantly lower freezing time percentage compared to the control group (Fig. 1F, I, and J). These findings collectively indicate that Mn exposure impairs cognitive function in mice.

To evaluate blood–brain barrier (BBB) integrity, we assessed brain microvascular permeability via tail vein injection of sodium fluorescein. Both cerebral cortex and hippocampus of Mn-treated mice displayed significantly increased sodium fluorescein fluorescence intensity (Fig. 1D and Fig. S1A right). Furthermore, tdTomato-Cdh5-Cre mice

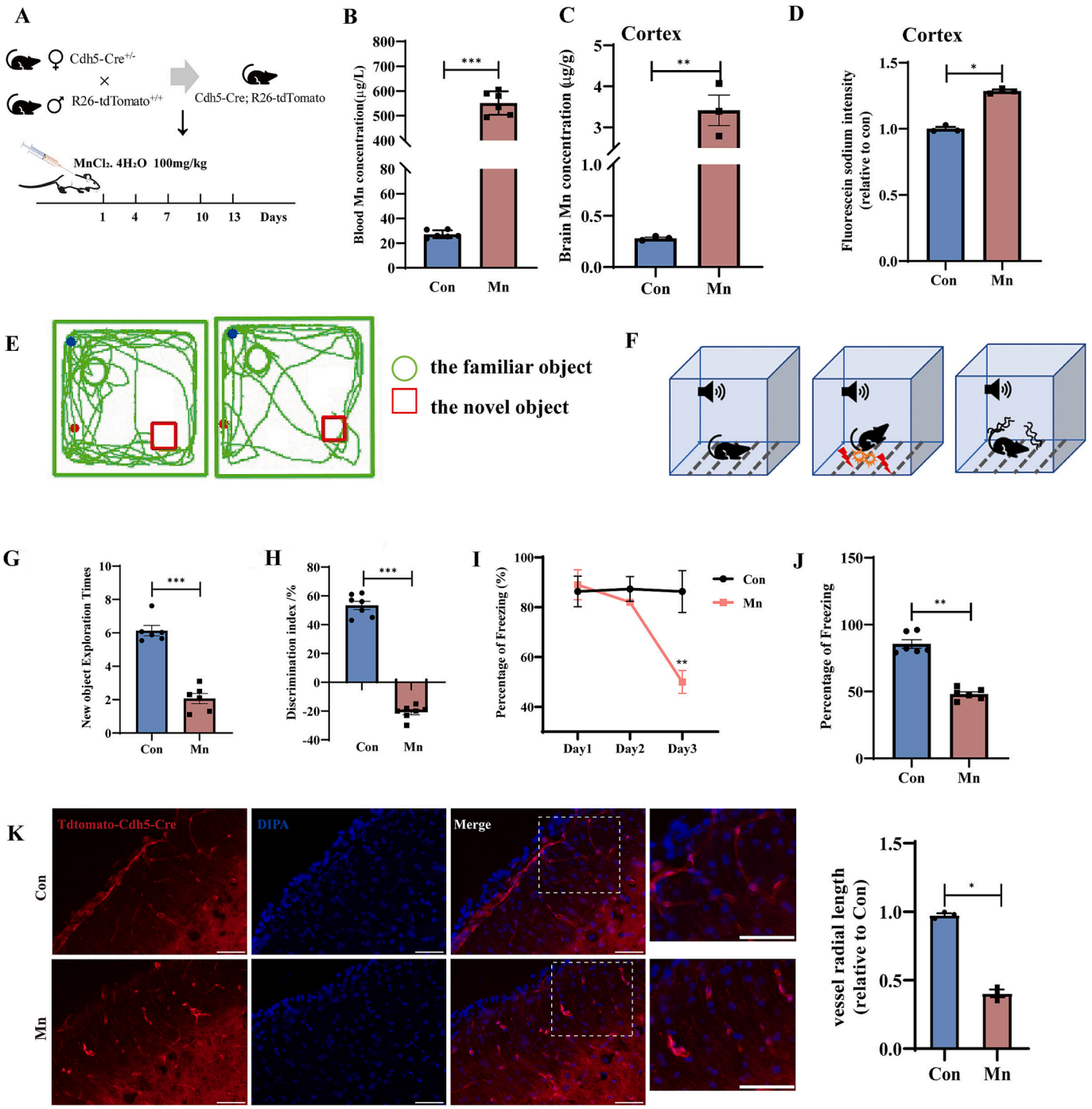

Fig. 1. Mn exposure reduces cognitive ability and increases BBB injury in mice. (A and B) Experiment schema of Mn treatment in mice. (C and D) Mn concentrations in blood (N = 6) and brain (N = 3). (E, F, G) Novel object recognition test. (H, I) Freezing behavior was expressed as percentage of time in the training and testing session for Mn (N = 6). (J) Fluorescence intensity of sodium fluorescein in cortex (N = 3). (K) Fluorescent signaling of blood vessels in the cerebral cortex of Cdh-5-Cre-tdTomato mice. Scale bars, 50 μm (N = 3). All graphs showed as mean ± SEM. *$p < 0.05$, **$p < 0.01$, ***$p < 0.001$ vs. Con. The same applies below.

were utilized to determine the extent of Mn-induced damage to BBB endothelial cells. A significant decrease in the radial length of cortical blood vessels was observed in the Mn-exposed group (Fig. 1K). These results demonstrate that Mn exposure leads to increased vascular injury and compromised BBB integrity in mice.

3.2. *Mn exposure decreases tight junction proteins in vitro and in vivo*

To investigate the effects of Mn exposure on tight junction proteins, we conducted both *in vitro* and *in vivo* studies. For the *in vitro* experiments, we utilized bEnd.3 cells, a brain microvascular endothelial cell line. Cell viability was assessed using MTT assays at various Mn concentrations and exposure times. No significant changes were observed after 24 h of exposure to 100 μM MnCl2 (Fig. S2). Subsequently, we employed this concentration (100 μM) for our *in vitro* experiments.

To evaluate cell permeability following Mn treatment, we used different molecular weights of FITC-dextran (Fluorescein 5-isothiocyanate-dextran). While small molecular weight dextran (4 kDa) can freely diffuse through cell membranes, large molecular weight dextran

(70 kDa), which mimics albumin *in vivo* (66 kDa), typically cannot pass through cell membranes under normal physiological conditions. Our results showed no effect of Mn exposure on the fluorescence intensity of small molecular weight FITC-dextran, but a significant increase in the fluorescence intensity of large molecular weight FITC-dextran (Fig. 2A and B). These findings indicate an increase in cell membrane permeability following Mn exposure.

Next, we analyzed tight junction proteins using both reverse-transcription polymerase chain reaction (RT-qPCR) and Western blot assays. RT-qPCR analysis revealed significant downregulation of ZO-1 and Ocln mRNA levels in Mn-treated bEnd.3 cells, while the expression of claudin-1 and claudin-2 remained unchanged (Fig. 2C). Western blot analysis confirmed a significant decrease in protein expression of ZO-1 and Ocln following Mn treatment (Fig. 2D and E). Furthermore, immunofluorescence staining demonstrated a significant decrease in the mean fluorescence intensity (MFI) of ZO-1 in Mn-exposed cells (Fig. 2F and 2G).We also examined TJP expression levels in brain tissues of Mn-exposed mice. RT-qPCR analysis showed significantly reduced ZO-1 and Ocln expression in both hippocampus and cortex tissues of Mn-exposed mice (Fig. 2H and Fig. S1C). Western blotting results corroborated these findings, revealing significantly reduced ZO-1 and Ocln protein levels in both cortical and hippocampal tissues of Mn-exposed mice compared to control mice (Fig. 2I and Fig. S1B). In conclusion, our research consistently demonstrates that Mn exposure leads to downregulated expression of tight junction proteins in both *in vitro* and *in vivo* models.

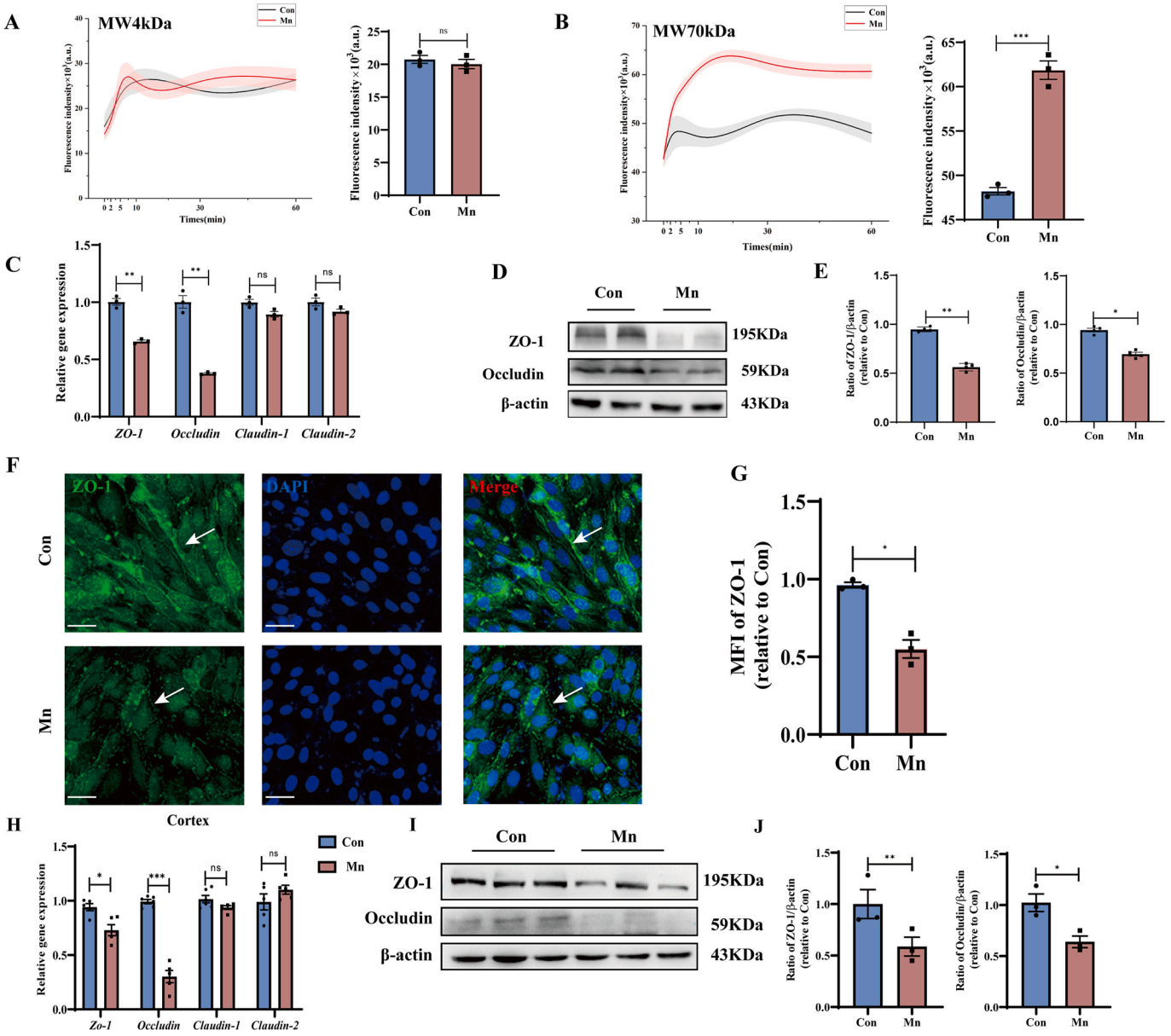

Fig. 2. Mn exposure decreases tight junction proteins *in vitro* and *in vivo*. (A and B) The permeability of bEnd.3 cell monolayer after Mn treatment. (C) The mRNA level of tight junction proteins. (D) Western blot gel images analysis of ZO-1 and Ocln expression *in vitro*. (E) Western blot assay revealed ZO-1 and Ocln protein expression. (N = 4). (F) Immunofluorescence staining red ZO-1 and blue DAPI in bEnd.3 cell. (N = 3). Scale bars, 100 μm. (G) The mean fluorescence intensity (MFI) of ZO-1 in bEnd.3 cells exposed to Mn was analyzed. (H) RT-qPCR assay of ZO-1, Ocln, claudin-1 and claudin-2 expression in cortex. (N = 4). (I) Western blot gel images of ZO-1 and Ocln expression level in cortex. (J) Western blot assay of protein expression of ZO-1 and Ocln quantification. (N = 3). All bar graphs showed as mean ± SEM. (For interpretation of the references to colour in this figure legend, the reader is referred to the web version of this article.)

3.3. Overexpression of Ocln (OE-Ocln) improves cognitive ability and increases blood–brain barrier tight junction protein expression in Mn exposed mice

To further elucidate the role of Occludin (Ocln) in manganese (Mn) toxicity, we employed a gene overexpression approach using adeno-associated virus (AAV) vectors. The experimental design involved administering either the AAV-overexpression-Ocln (OE-Ocln) vector or a control vector (AAV-control, NC) to tdTomato-Cdh5-Cre mice (Fig. 3A). Following Mn exposure, we conducted a series of behavioral tests and biochemical analyses to assess the effects of Ocln overexpression.

Consistent with previous findings, blood Mn levels increased significantly after Mn exposure in all treated groups (Fig. 3B). Interestingly, the Mn concentration in brain tissue, particularly in the cortex region, was significantly reduced in the OE-Ocln + Mn group compared to the NC + Mn group (Fig. 3C). This suggests that Ocln overexpression may play a role in reducing Mn accumulation in the brain.

Behavioral testing revealed notable differences between the experimental groups. In the novel object recognition test, Mn-treated mice generally exhibited reduced exploration of new objects. However, the discrimination index was significantly higher in the OE-Ocln + Mn group compared to the NC + Mn group (Fig. 3D-F), indicating improved cognitive function with Ocln overexpression. Morphological analysis of the cortical vasculature showed that the OE-Ocln + Mn group had a significantly increased radial length of blood vessels compared to the NC + Mn group (Fig. 3G). This observation suggests that Ocln overexpression may promote vascular development or maintenance in the presence of Mn toxicity. To investigate the molecular mechanisms underlying these effects, we examined changes in TJPs in the mouse cortex using RT-PCR and Western blot analyses. The results demonstrated that OE-Ocln + Mn treatment significantly elevated the expression of Ocln at both mRNA and protein levels. Interestingly, no significant changes were observed for the ZO-1 protein compared to the NC + Mn group (Fig. 3H and I). This selective upregulation of Ocln suggests a specific role for this protein in mediating the protective effects against Mn toxicity.

Collectively, these findings indicate that overexpression of Ocln can alleviate cognitive impairment and enhance the expression of the tight junction protein Ocln in mice exposed to manganese. Further research is warranted to elucidate the precise mechanisms by which Ocln exerts these protective effects and to explore potential therapeutic applications in managing Mn-related disorders.

3.4. Gastrodin (GAS) protects the BBB and alleviates cognitive dysfunction in Mn-exposed mice

To investigate the potential of GAS in preventing cognitive impairment induced by manganese (Mn) exposure in mice, we conducted a comprehensive study using a well-designed experimental protocol (Fig. 4A). Upon completion of the treatment regimen, cognitive function was assessed using behavioral tests, including fear conditioning and novel object recognition tests. Blood Mn levels were quantified across different treatment groups using atomic absorption spectrometry. The Mn-exposed group exhibited significantly elevated blood Mn levels compared to the control group. Notably, the GAS treatment resulted in a marked reduction of Mn levels in the blood of Mn-exposed mice (Fig. 4B). Further analysis of Mn concentration in the cortex and hippocampus revealed significant decreases in Mn levels following GAS treatment, relative to the Mn-exposed group (Fig. 4C and Fig. S3A). In the fear conditioning experiment, no significant differences in freezing time percentages were observed among the Mn, Con, GAS, and GAS + Mn groups during the initial conditioning stage. However, on the second day (contextual test, Fig. 4H) and third day (cue test, Fig. 4J), the GAS + Mn group demonstrated increased freezing time percentages compared to the Mn treatment group, indicating improved cognitive function.

To assess blood–brain barrier (BBB) integrity, we administered intravenous fluorescein sodium. The Mn + GAS group exhibited notably reduced fluorescent intensity in both cortex and hippocampus tissues compared to the Mn-exposed group (Fig. 4D and Fig. S3B). Collectively, these data provide evidence for the protective effects of GAS against Mn-induced cognitive impairment in mice, potentially through the preservation of BBB integrity and reduction of Mn accumulation in the brain.

3.5. GAS protects against BBB damage induced by Mn treatment through upregulation of TJPs expression

To investigate the protective effects of GAS on BBB integrity after Mn exposure, we examined the expression of ZO-1 and Ocln both *in vivo* and *in vitro*. In the *in vivo* study, RT-qPCR and Western blot (WB) assays were performed to detect ZO-1 and Ocln expression in mouse brain tissues (hippocampus and cortex). Intragastric administration of GAS significantly reversed the Mn-induced decrease in mRNA expression of both ZO-1 and Ocln (Fig. S2D and E). At the protein level, WB analysis revealed that GAS treatment alleviated the Mn-induced decline in Ocln protein expression in cortex tissues (Fig. 4K-L). A similar effect was observed for ZO-1 protein expression. Comparable results were also found in the hippocampus (Fig. S3C).

To further validate these findings, we conducted additional experiments using bEnd.3 cells, an *in vitro* model of the BBB. Initially, we assessed the effect of GAS on cell viability to determine the optimal concentration for treatment. GAS concentrations below 100 μM showed no significant impact on cell viability (Fig. 5A). Subsequently, bEnd.3 cells were treated with 10, 20, and 50 μM of GAS. The results demonstrated that 20 μM GAS effectively mitigated the Mn-induced decrease in ZO-1 and Ocln mRNA levels (Fig. 5B). Based on these findings, 20 μM GAS was selected for subsequent experiments.

To determine whether protein levels were similarly affected, we performed WB experiments. Treatment with Mn alone caused a significant decrease in ZO-1 protein expression, while the addition of 20 μM GAS increased the expression of both ZO-1 and Ocln compared to the Mn-treated group (Fig. 5C). To assess the functional implications of these changes, we conducted permeability assays using FITC-dextran. While no significant difference was observed in the permeability of small molecular weight FITC-dextran (4 kDa) (Fig. 5D), treatment with 20 μM GAS significantly reduced the Mn-induced increase in bEnd.3 cell permeability to large molecular weight FITC-dextran (70 kDa) (Fig. 5E). Collectively, these results suggest that GAS protects against BBB damage induced by Mn treatment by upregulating the expression of tight junction proteins, thereby maintaining BBB integrity.

3.6. GAS inhibits the RhoA/ROCK2 pathway in Mn-treated bEnd.3 cells

To investigate the effects of manganese (Mn) exposure on this pathway, we examined the protein expression of RhoA and ROCK isoforms in Mn-treated bEnd.3 cells using Western blot analysis. Our results, as illustrated in Fig. 6A and B, demonstrate that Mn treatment significantly upregulated the expression of RhoA and ROCK2 proteins, while ROCK1 protein levels remained unchanged compared to the control. These findings suggest that Mn exposure activates the RhoA/ROCK2 signaling pathway. Given the established importance of the Rho/ROCK pathway in modulating cytoskeleton-based functions, including cell morphology, migration, adhesion, and barrier function (both epithelial and blood–brain), we sought to determine the potential inhibitory effects of gastrodin (GAS) on the Mn-activated RhoA/ROCK2 signaling pathway. Treatment with GAS resulted in significantly attenuated changes in RhoA and ROCK2 protein levels (Fig. 6C and D). To further elucidate the relationship between the RhoA/ROCK2 pathway and tight junction proteins (TJPs), we conducted *in vitro* experiments using HA-1077, a potent inhibitor of the RhoA/ROCK signaling pathway (Fig. 6E and F). Western blot analysis revealed that HA-1077 significantly downregulated the protein expression of both RhoA and ROCK2 following Mn intoxication. Subsequently, we examined the expression of

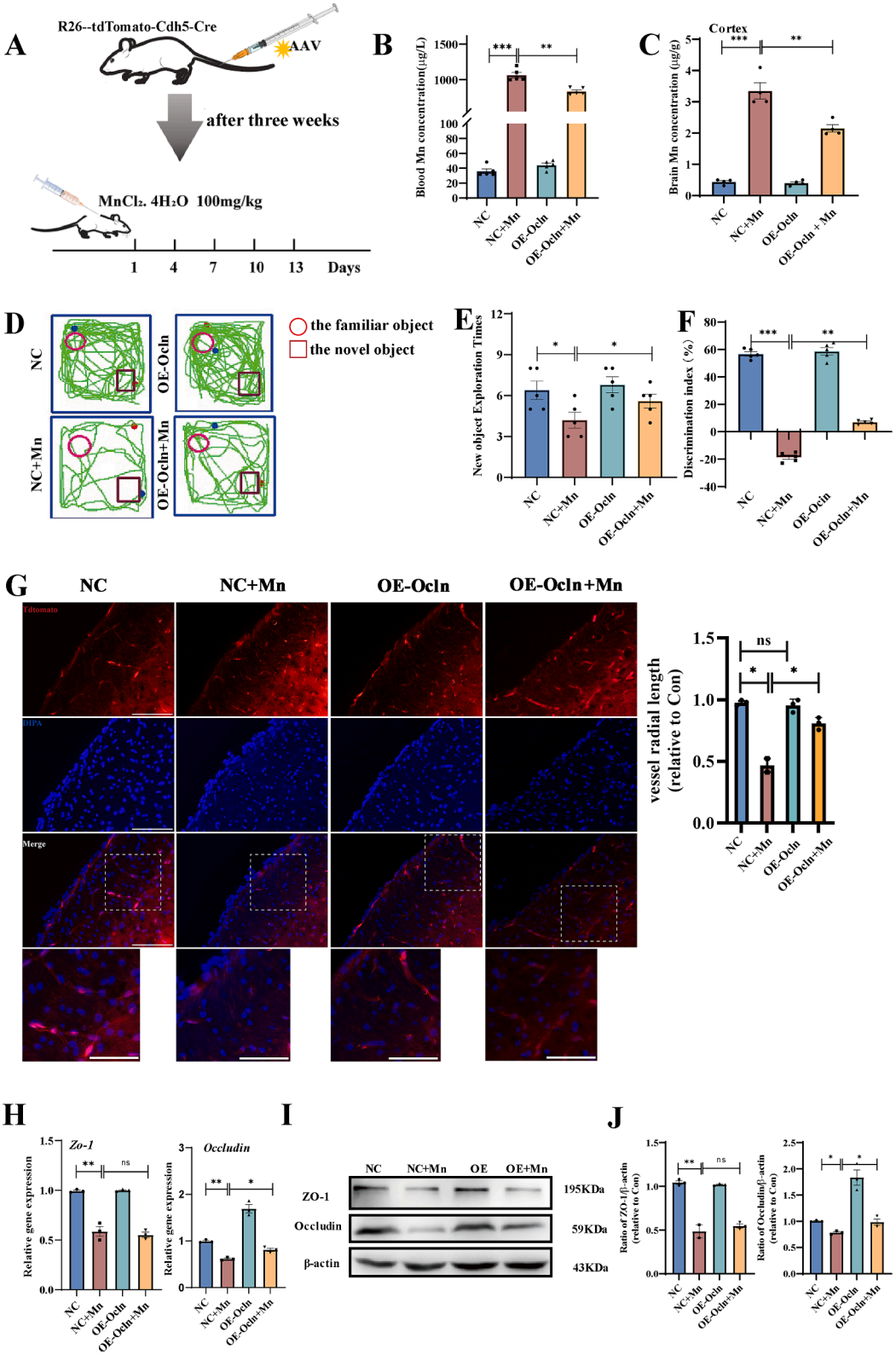

Fig. 3. Overexpression of Ocln (OE-Ocln) improves the Mn-induced impaired cognition and increased the expression of tight junction proteins of the blood–brain barrier. (A) The sketch map showed the processes of Mn exposure in this study. (B) and (C) Mn concentrations in blood and brain of tdTomato-Cdh5-Cre mice with tail vein injected AAV-Cdh5-NC or AAV-Ocln OE. (N = 3) (D, E and F) Novel object recognition test in Mn-exposed mice. (E) The time of new object exploration. (F) New object recognition experiment discrimination index. (N = 5). (G) The fluorescence signs of blood vessels in the cerebral cortex of Cdh-5-Cre-tdTomato mice. Scale bar, 50 μm. (H) The qRT-PCR analyzed the level of tight junction proteins in cortex. (I) Western blot gel images of ZO-1 and Ocln expression in cortex. (J) Quantification of western blot analysis of ZO-1 and Ocln proteins. (N = 3) Graphs show group mean ± SEM.

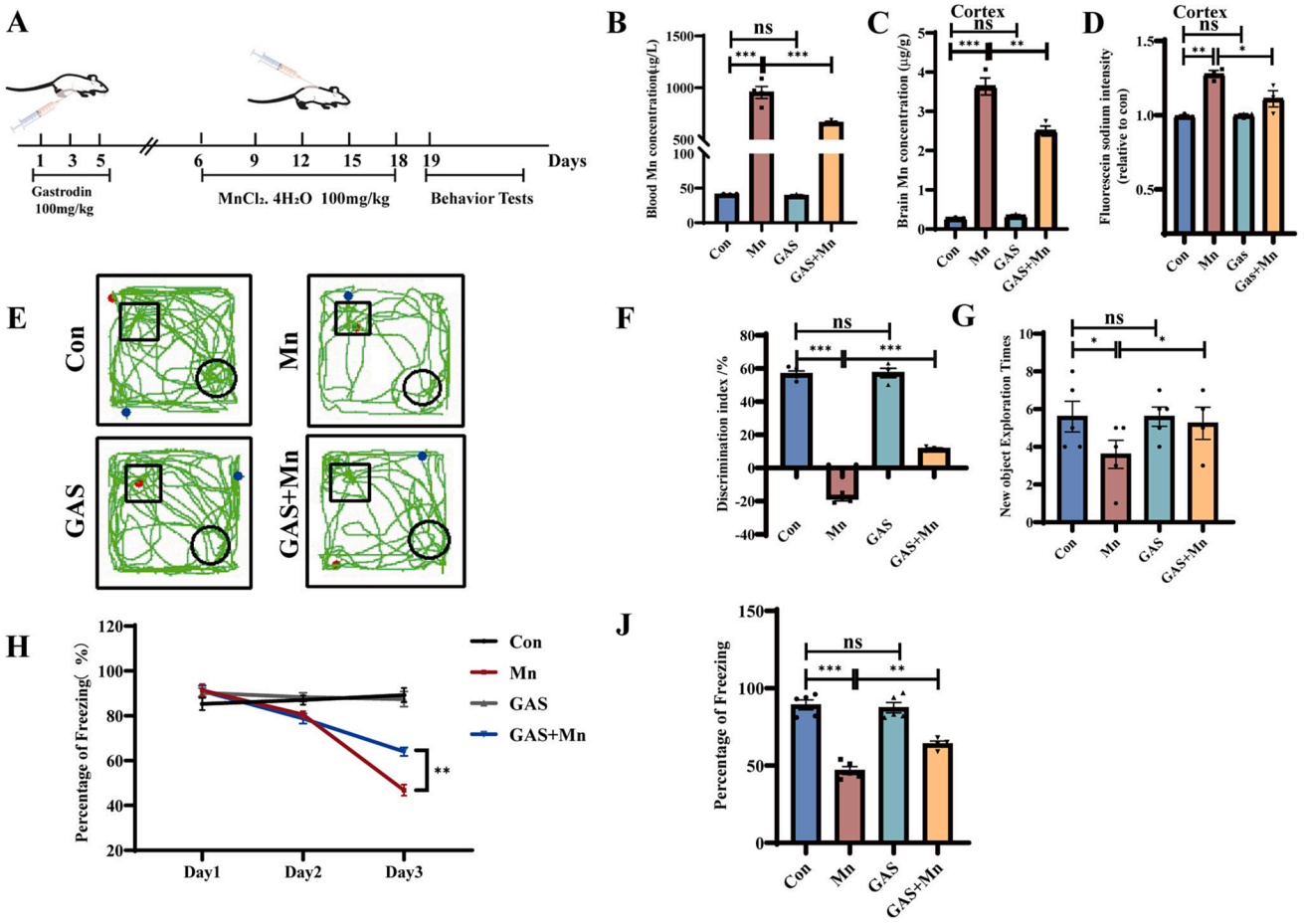

Fig. 4. Gastrodin (GAS) reverses the BBB effects and alleviates the cognitive dysfunction induced by Mn in mice. (A) Schematic diagram of the experiment. (B, C) Mn levels detected in the blood and brain (N = 3). (D) Amount of sodium fluorescein measured in the cortex of the brain (N = 3). (E, F and G, H) Multiple forms of cognition were tested for. (F and G) Amount of time Mn treated mice will explore objects during the novel object recognition test. (F) Percentage of discrimination. (G) Freezing behavior of the mice treated with Mn during the training and testing sessions represented as a percentage of time (N = 5). Data are mean ± SEM. Significant differences were analyzed using Two-way ANOVA.

cellular TJPs after suppressing the RhoA/ROCK pathway. Our findings demonstrated that HA-1077 treatment significantly upregulated ZO-1 and Ocln proteins compared to Mn-exposed cells. Based on these results, we postulate that GAS may mitigate Mn toxicity through the inhibition of the RhoA/ROCK2 pathway.

In conclusion, our study provides evidence for the protective effects of GAS against Mn-induced toxicity, potentially mediated through the modulation of the RhoA/ROCK2 signaling pathway and subsequent preservation of tight junction integrity.

4. Discussion

Mn is an essential trace element for the human body, playing a crucial role in various physiological processes. However, excessive Mn exposure can lead to neurotoxicity and damage to the CNS (Wang et al., 2017). The BBB is a critical component in maintaining CNS homeostasis and has been implicated in several neurodegenerative disorders, including Alzheimer's disease (AD), Parkinson's disease (PD), and Huntington's disease (HD) (Huang et al., 2020; Iyer et al., 2021). In this study, we found that Mn exposure could lead to the increase of BBB permeability and the decline of learning and memory ability in mice. We found that tight junction proteins played an important role in the increase of BBB permeability induced by Mn exposure. In addition, the protection of BBB by GAS could alleviate the damage caused by Mn exposure in mice, and the RhoA/Rock2 signaling pathway may be involved.

The primary routes by which Mn enters the brain microenvironment include transport across the BBB, absorption through inhaled cerebrospinal fluid (CSF), and passage through the blood-cerebrospinal fluid barrier (Horning et al., 2015; McCabe & Zhao, 2021). The BBB serves as a critical regulatory interface within the CNS, tightly controlling the microenvironment. The BBB is mainly composed of endothelial cells, astrocytes, microglia and pericytes. Numerous previous studies have shown that manganese-induced neurotoxicity leads to significant activation of astrocytes and microglia and expression of many neuroinflammatory genes, which aggravates neuronal damage (Kisler et al., 2017). The results also suggest that microglia are activated after Mn exposure and that the neuroinflammation mediated by microglia is involved in the pathological mechanism of the body (Kirkley et al., 2017). Studies have shown that manganese can activate microglia and increase the release of proinflammatory cytokines, leading to damage to dopaminergic neurons in the brain of rats (Zhao et al., 2009). Mn exposure dysfunctions mitochondrial biology in astrocytes, leading to the release of proinflammatory cytokines and adjacent neuronal damage (Sarkar et al., 2018). The endothelium also plays a key role in regulating the entry of immune cells and molecules into the CNS. Normally, the BBB tightly controls the entry of substances to protect the neuronal environment (Abbott et al., 2006). However, during neuroinflammation, activated endothelial cells can increase the permeability of the BBB, thereby allowing immune cells and inflammatory mediators to enter the brain (Oliveira-Paula et al., 2024). It is composed of capillary endothelial cells expressing TJPs that form a highly selective barrier

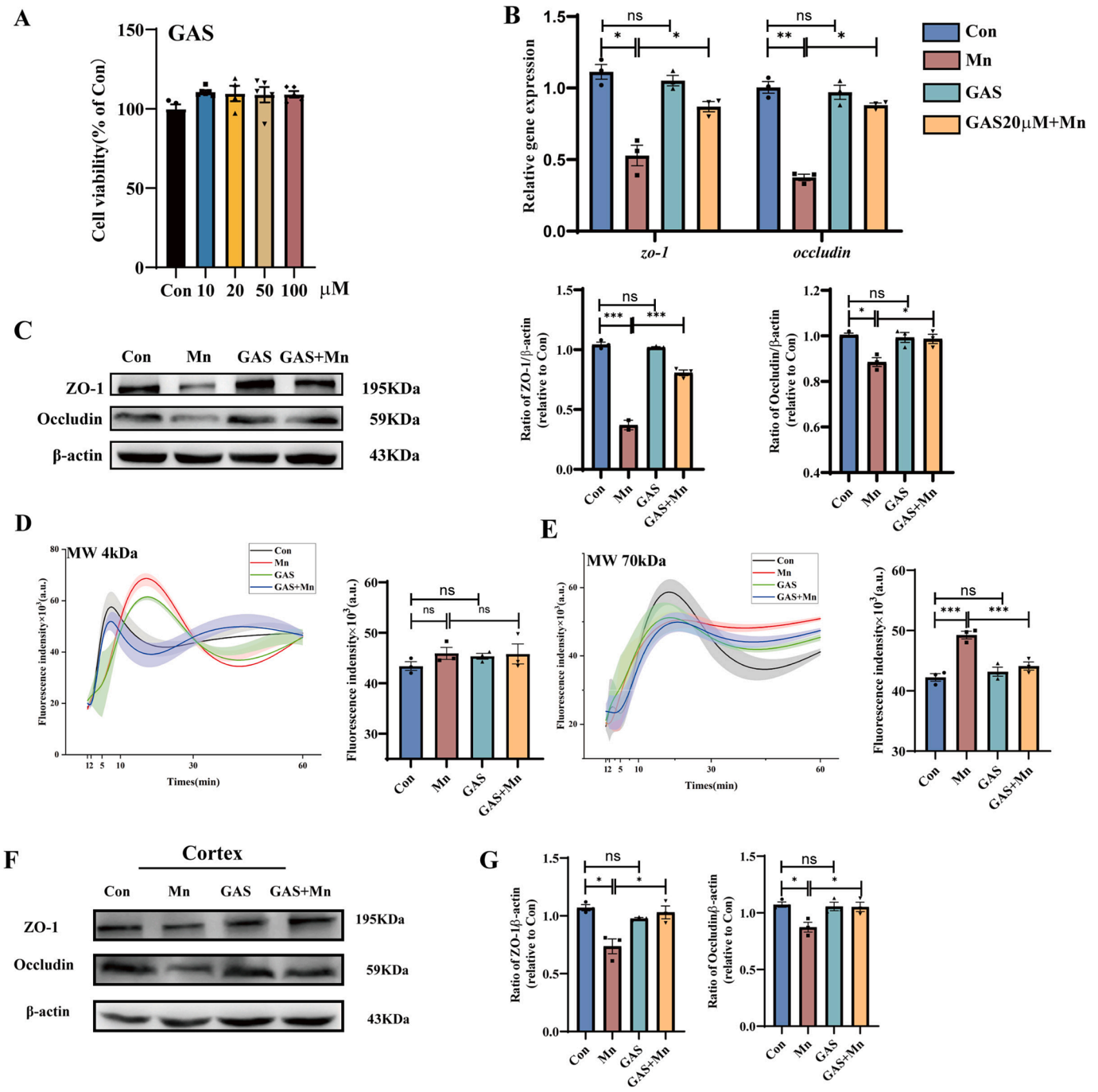

Fig. 5. GAS protects against BBB damage after Mn treatment by increasing TJPs expression *in vitro* and *in vivo*. (A) Cell viabilities of bEnd.3 cells were analyzed by MTT assay when exposed to GAS at indicated doses. N = 6. (B) RT-qPCR was used to measure the mRNA levels of ZO-1 and Ocln in bEnd.3 cells after GAS treatment. (C) The protein levels of ZO-1 and Ocln in bEnd.3 cells were determined by Western blot. (D and E) Transwell assay was used to determine the permeability of FITC across the monolayer of bEnd.3 cells with or without GAS treatment. (F) In the cortex, Western blot assay was used to measure the protein levels of ZO-1 and Ocln. (G) Quantification of Western blot analysis in cortex was obtained. (N = 3). Data are reported as mean ± SEM.

between the blood and brain parenchyma (Crossgrove & Zheng, 2004). TJPs, including Ocln, Claudin-5, and ZO-1, are major structural components of the BBB (Willis et al., 2004). Alterations in TJP expression, localization, or post-translational modifications can significantly impact BBB function (Burek et al., 2019). BBB dysfunction has been associated with various neuropathologies, potentially triggering a cascade of events including neuroinflammation, disruption of ion homeostasis, matrix metalloproteinase activation, aberrant synaptogenesis, and pathological synaptic plasticity (David et al., 2009; Kim et al., 2017; Levy et al., 2015; Salar et al., 2016; Weissberg et al., 2015). Recent studies have identified BBB disruption as an early biomarker for cognitive dysfunction in humans (Nation et al., 2019). Furthermore, BBB dysfunction in AD has been linked to alterations in brain endothelial cells, which can be mitigated through targeted regulation of the Wnt/β-catenin signaling pathway, suggesting a potential therapeutic approach (Wang et al., 2022). Our research corroborates these findings, demonstrating that excessive Mn exposure leads to a significant reduction in TJPs ZO-1 and Ocln at both mRNA and protein levels. Under normal physiological conditions, Mn homeostasis is regulated by various transport proteins, including divalent metal ion transporter protein 1 (DMT1, SLC11A2),

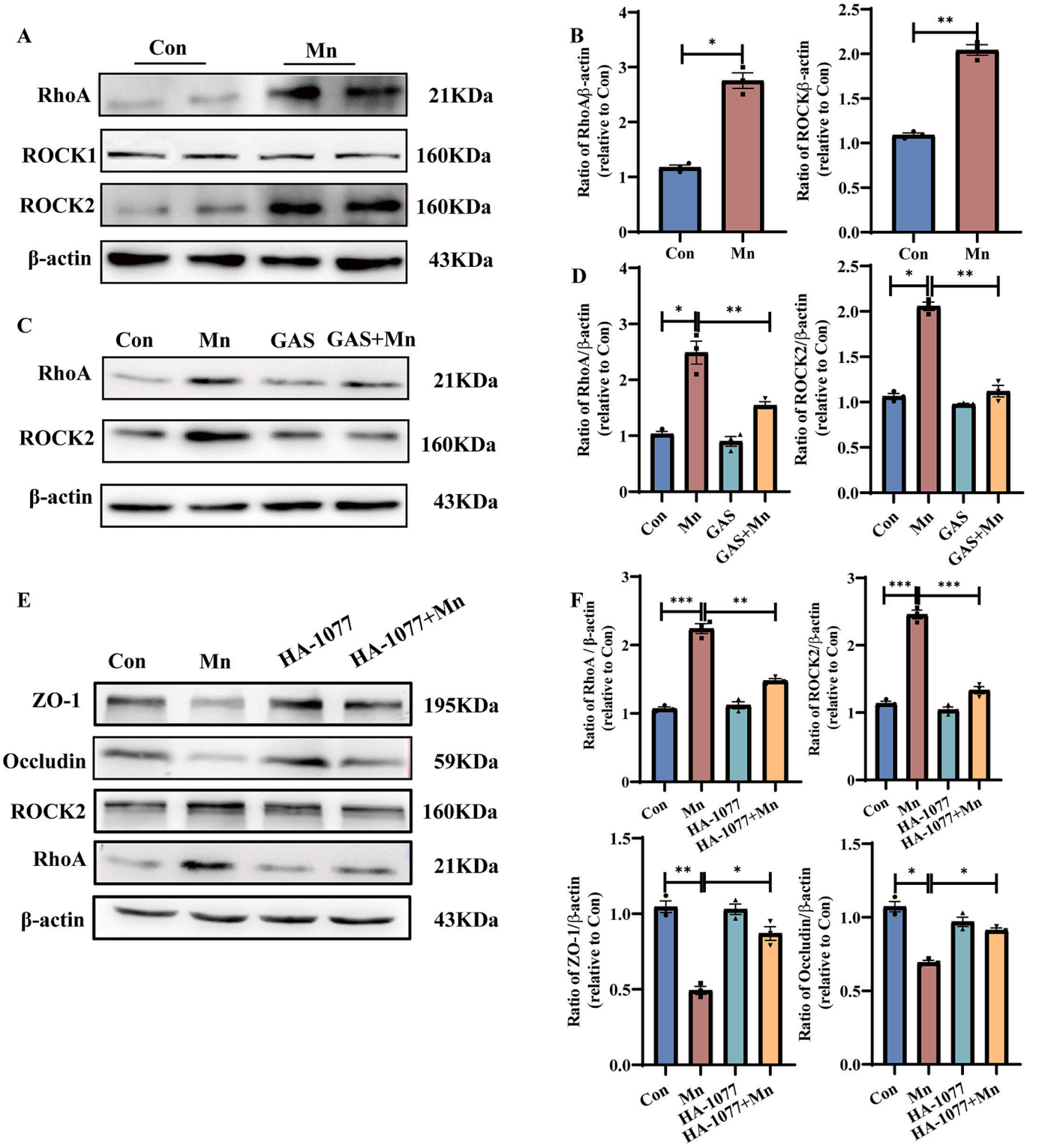

Fig. 6. GAS inhibited the RhoA/ROCK pathway in Mn-treated bEnd.3 cells. (A, C) The expression of RhoA and ROCK protein was assessed by western blotting (B) Quantitative analysis of protein bands. The student's *t*-test. (N = 4). (D) Quantitative analysis of protein bands. (E–F) bEnd.3 cells were treated with or without RhoA/ROCK inhibitor (HA-1077, 25 μM) 2 h before Mn treatment. (E) Protein levels of ZO-1, Ocln, RhoA and ROCK2 were measured by western blotting. (F) Gray analysis of protein expression. These comparisons were carried out using ANOVA with the post-hoc Tukey test (N = 4).

and metal cation cotransport proteins ZIP8 (SLC39A8) and ZIP14 (SLC39A14) (Chen et al., 2015). However, our experiments revealed that excess Mn did not alter DMT1 expression, suggesting alternative mechanisms of Mn-induced neurotoxicity. Our findings demonstrate that excessive Mn exposure results in altered BBB permeability, decreased TJP expression, and increased neurotoxicity, although the precise mechanisms underlying these effects require further investigation.

Small molecule drugs play a crucial role in BBB protection due to their ability to penetrate the BBB. For instance, Zebularine has been

shown to protect against BBB disruption by increasing the expression of ZO-1 and vascular endothelial (VE)-cadherin, while catalpol demonstrates protective effects against fibrillar Amyloid-β (1–42)-induced BBB disruption (Mo et al., 2021; Yang et al., 2021). Resveratrol, a polyphenolic compound, has been observed to restore neuronal TJPs (Vairappan et al., 2019). Resveratrol, a polyphenolic compound, has been observed to restore neuronal TJPs (Bavarsad et al., 2019). Gastrodin (GAS), upon entering systemic circulation, rapidly distributes and concentrates in the central nervous system, exerting a protective effect (Liu et al., 2018; Zhan et al., 2016). Xiao et al. reported that GAS exhibited memory-enhancing effects by promoting hippocampal neurogenesis in memory-impaired mice. Furthermore, GAS has shown efficacy in treating neuroinflammation induced by lipopolysaccharide (LPS) in rats and can protect cognitive and memory abilities in patients with cognitive impairment (Wu et al., 2019). GAS has also been found to enhance the function of endothelial cells through increased expression of tight junction proteins (Li et al., 2021a). Moreover, GAS demonstrated anxiolytic action through the RhoA/ROCK signaling pathway (Chen et al., 2016). In our experiment, we observed that GAS can alleviate cognitive injury induced by manganese (Mn), mitigate BBB damage, and reverse the inhibition of the RhoA/ROCK pathway. RhoA, a member of the Rho family of small GTPases, regulates various signaling pathways and influences diverse cellular functions. In the CNS, Rho GTPases play a vital role in brain development (Zamboni et al., 2018). RhoA mediates cytoskeleton formation and cytokinesis (Naydenov et al., 2021). In neurological diseases, RhoA/ROCK signaling is particularly important in regulating cytoskeletal dynamics (Roser et al., 2017). hoA specifically binds to the TJPs and exerts a protective effect (Jaiswal et al., 2011). Additionally, our study confirmed that Mn can affect the expression of TJPs (Occludin, ZO-1) through activation of the RhoA/ROCK2 signaling pathway.

In conclusion, our study revealed that Mn causes BBB damage and decreases the expression of tight junction proteins, which has never been demonstrated in previous studies. GAS, as a protective agent of the barrier system, can attenuate Mn-induced BBB damage, and thus, may attenuate cognitive deficits caused by Mn toxicity. We propose that future studies should further elucidate the therapeutic modalities of GAS and the mechanisms involved in the alteration of BBB permeability in neurodegenerative diseases characterized by cognitive dysfunction.

5. Conclusions

This new study provides evidence that GAS ameliorates cognitive impairment and attenuates altered tight junction protein permeability following Mn exposure via the RhoA/ROCK2 pathway in bEnd.3 cells.

CRediT authorship contribution statement

Yan Ma: Conceptualization, Methodology, Validation, Formal analysis, Investigation, Resources, Data curation, Writing – original draft, Visualization. **Honggang Chen:** Resources, Investigation. **Yuxin Jiang:** Formal analysis, Data curation, Visualization. **Diya Wang:** Resources, Investigation. **Michael Aschner:** Supervision. **Wenjing Luo:** Conceptualization, Supervision. **Peng Su:** Conceptualization, Methodology, Writing – review & editing, Supervision.

Declaration of competing interest

The authors declare that they have no known competing financial interests or personal relationships that could have appeared to influence the work reported in this paper.

Acknowledgements

This work was supported by the International Cooperation and Exchange Program of the National Natural Science Foundation of China (82020108026) and Shaanxi Provincial Major Project (2024JC-YBMS-708).

Appendix A. Supplementary data

Supplementary data to this article can be found online at https://doi.org/10.1016/j.crtox.2024.100207.

Data availability

All data that support the findings of this study are included in this manuscript and its Supplementary Information Files.

References

Abbott, N.J., Ronnback, L., Hansson, E., 2006. Astrocyte-endothelial interactions at the blood-brain barrier. *Nat. Rev. Neurosci.* 7 (1), 41–53. https://doi.org/10.1038/nrn1824.

Balachandran, R.C., Mukhopadhyay, S., McBride, D., Veevers, J., Harrison, F.E., Aschner, M., Bowman, A.B., 2020. Brain manganese and the balance between essential roles and neurotoxicity. *J. Biol. Chem.* 295 (19), 6312–6329. https://doi.org/10.1074/jbc.REV119.009453.

Bavarsad, K., Barreto, G.E., Hadjzadeh, M.A., Sahebkar, A., 2019. Protective effects of curcumin against ischemia-reperfusion injury in the nervous system. *Mol. Neurobiol.* 56 (2), 1391–1404. https://doi.org/10.1007/s12035-018-1169-7.

Burek, M., Konig, A., Lang, M., Fiedler, J., Oerter, S., Roewer, N., Forster, C.Y., 2019. Hypoxia-induced MicroRNA-212/132 alter blood-brain barrier integrity through inhibition of tight junction-associated proteins in human and mouse brain microvascular endothelial cells. *Transl. Stroke Res.* 10 (6), 672–683. https://doi.org/10.1007/s12975-018-0683-2.

Chen, P., Chakraborty, S., Mukhopadhyay, S., Lee, E., Paoliello, M.M., Bowman, A.B., Aschner, M., 2015. Manganese homeostasis in the nervous system. J. Neurochem. 134 (4), 601–610. https://doi.org/10.1111/jnc.13170.

Chen, W.C., Lai, Y.S., Lin, S.H., Lu, K.H., Lin, Y.E., Panyod, S., Sheen, L.Y., 2016. Antidepressant effects of Gastrodia elata Blume and its compounds gastrodin and 4-hydroxybenzyl alcohol, via the monoaminergic system and neuronal cytoskeletal remodeling. *J. Ethnopharmacol.* 182, 190–199. https://doi.org/10.1016/j.jep.2016.02.001.

Crossgrove, J., Zheng, W., 2004. Manganese toxicity upon overexposure. *NMR Biomed.* 17 (8), 544–553. https://doi.org/10.1002/nbm.931.

David, Y., Cacheaux, L.P., Ivens, S., Lapilover, E., Heinemann, U., Kaufer, D., Friedman, A., 2009. Astrocytic dysfunction in epileptogenesis: consequence of altered potassium and glutamate homeostasis? *J. Neurosci.* 29 (34), 10588–10599. https://doi.org/10.1523/JNEUROSCI.2323-09.2009.

Guilarte, T.R., 2013. Manganese neurotoxicity: new perspectives from behavioral, neuroimaging, and neuropathological studies in humans and non-human primates. *Front. Aging Neurosci.* 5, 23. https://doi.org/10.3389/fnagi.2013.00023.

He, J., Li, X., Yang, S., Li, Y., Lin, X., Xiu, M., Liu, Y., 2021. Gastrodin extends the lifespan and protects against neurodegeneration in the Drosophila PINK1 model of Parkinson's disease. *Food Funct.* 12 (17), 7816–7824. https://doi.org/10.1039/d1fo00847a.

Horning, K.J., Caito, S.W., Tipps, K.G., Bowman, A.B., Aschner, M., 2015. Manganese is essential for neuronal health. *Annu. Rev. Nutr.* 35, 71–108. https://doi.org/10.1146/annurev-nutr-071714-034419.

Huang, Z., Wong, L.W., Su, Y., Huang, X., Wang, N., Chen, H., Yi, C., 2020. Blood-brain barrier integrity in the pathogenesis of Alzheimer's disease. *Front. Neuroendocrinol.* 59, 100857. https://doi.org/10.1016/j.yfrne.2020.100857.

Iyer, M., Subramaniam, M.D., Venkatesan, D., Cho, S.G., Ryding, M., Meyer, M., Vellingiri, B., 2021. Role of RhoA-ROCK signaling in Parkinson's disease. *Eur. J. Pharmacol.* 894, 173815. https://doi.org/10.1016/j.ejphar.2020.173815.

Jaiswal, M., Gremer, L., Dvorsky, R., Haeusler, L.C., Cirstea, I.C., Uhlenbrock, K., Ahmadian, M.R., 2011. Mechanistic insights into specificity, activity, and regulatory elements of the regulator of G-protein signaling (RGS)-containing Rho-specific guanine nucleotide exchange factors (GEFs) p115, PDZ-RhoGEF (PRG), and Leukemia-associated RhoGEF (LARG). *J. Biol. Chem.* 286 (20), 18202–18212. https://doi.org/10.1074/jbc.M111.226431.

Jiang, G., Hu, Y., Liu, L., Cai, J., Peng, C., Li, Q., 2014. Gastrodin protects against MPP(+)-induced oxidative stress by up regulates heme oxygenase-1 expression through p38 MAPK/Nrf2 pathway in human dopaminergic cells. *Neurochem. Int.* 75, 79–88. https://doi.org/10.1016/j.neuint.2014.06.003.

Kim, S.Y., Senatorov, V.V., Morrissey, C.S., Lippmann, K., Vazquez, O., Milikovsky, D.Z., . . . Kaufer, D. (2017). TGFβ signaling is associated with changes in inflammatory gene expression and perineuronal net degradation around inhibitory neurons following various neurological insults. *Sci. Rep 7*. doi: ARTN 7711 10.1038/s41598-017-07394-3.

Kim, K.A., Kim, D., Kim, J.H., Shin, Y.J., Kim, E.S., Akram, M., Bae, O.N., 2020. Autophagy-mediated occludin degradation contributes to blood-brain barrier disruption during ischemia in bEnd.3 brain endothelial cells and rat ischemic stroke models. *Fluids Barriers CNS* 17 (1), 21. https://doi.org/10.1186/s12987-020-00182-8.

Kirkley, K.S., Popichak, K.A., Afzali, M.F., Legare, M.E., Tjalkens, R.B., 2017. Microglia amplify inflammatory activation of astrocytes in manganese neurotoxicity. *J. Neuroinflammation* 14 (1), 99. https://doi.org/10.1186/s12974-017-0871-0.

Kisler, K., Nelson, A.R., Rege, S.V., Ramanathan, A., Wang, Y.M., Ahuja, A., Zlokovic, B. V., 2017. Pericyte degeneration leads to neurovascular uncoupling and limits oxygen supply to brain. *Nat. Neurosci.* 20 (3), 406–416. https://doi.org/10.1038/nn.4489.

Levy, N., Milikovsky, D.Z., Baranauskas, G., Vinogradov, E., David, Y., Ketzef, M., Monsonego, A., 2015. Differential TGF-beta signaling in glial subsets underlies IL-6-mediated epileptogenesis in mice. *J. Immunol.* 195 (4), 1713–1722. https://doi.org/10.4049/jimmunol.1401446.

Li, S., Bian, L., Fu, X., Ai, Q., Sui, Y., Zhang, A., Lu, D., 2019. Gastrodin pretreatment alleviates rat brain injury caused by cerebral ischemic-reperfusion. *Brain Res.* 1712, 207–216. https://doi.org/10.1016/j.brainres.2019.02.006.

Li, J., Huang, J., He, Y., Wang, W., Leung, C.K., Zhang, D., Li, Z., 2021a. The protective effect of gastrodin against the synergistic effect of HIV-Tat protein and METH on the blood-brain barrier via glucose transporter 1 and glucose transporter 3. *Toxicol. Res. (Camb)* 10 (1), 91–101. https://doi.org/10.1093/toxres/tfaa102.

Li, J., Pang, S.Y., Wang, Z., Guo, Q., Duan, J., Sun, S., Jiang, J., 2021b. Oxidative transformation of emerging organic contaminants by aqueous permanganate: kinetics, products, toxicity changes, and effects of manganese products. *Water Res.* 203, 117513. https://doi.org/10.1016/j.watres.2021.117513.

Liu, Y., Gao, J., Peng, M., Meng, H., Ma, H., Cai, P., Si, G., 2018. A review on central nervous system effects of gastrodin. *Front. Pharmacol.* 9, 24. https://doi.org/10.3389/fphar.2018.00024.

McCabe, S.M., Zhao, N., 2021. The potential roles of blood-brain barrier and blood-cerebrospinal fluid barrier in maintaining brain manganese homeostasis. *Nutrients* 13 (6). https://doi.org/10.3390/nu13061833.

Mo, Y., Yue, E., Shi, N., Liu, K., 2021. The protective effects of curcumin in cerebral ischemia and reperfusion injury through PKC-theta signaling. *Cell Cycle* 20 (5–6), 550–560. https://doi.org/10.1080/15384101.2021.1889188.

Nation, D.A., Sweeney, M.D., Montagne, A., Sagare, A.P., D'Orazio, L.M., Pachicano, M., Zlokovic, B.V., 2019. Blood-brain barrier breakdown is an early biomarker of human cognitive dysfunction. *Nat. Med.* 25 (2), 270. https://doi.org/10.1038/s41591-018-0297-y.

Naydenov, N.G., Koblinski, J.E., Ivanov, A.I., 2021. Anillin is an emerging regulator of tumorigenesis, acting as a cortical cytoskeletal scaffold and a nuclear modulator of cancer cell differentiation. *Cell. Mol. Life Sci.* 78 (2), 621–633. https://doi.org/10.1007/s00018-020-03605-9.

Ojemann, L.M., Nelson, W.L., Shin, D.S., Rowe, A.O., Buchanan, R.A., 2006. Tian ma, an ancient Chinese herb, offers new options for the treatment of epilepsy and other conditions. *Epilepsy Behav.* 8 (2), 376–383. https://doi.org/10.1016/j.yebeh.2005.12.009.

Oliveira-Paula, G.H., Martins, A.C., Ferrer, B., Tinkov, A.A., Skalny, A.V., Aschner, M., 2024. The impact of manganese on vascular endothelium. *Toxicol. Res.* 40 (4), 501–517. https://doi.org/10.1007/s43188-024-00260-1.

Peng, Z., Wang, H., Zhang, R., Chen, Y., Xue, F., Nie, H., Tan, Q., 2013. Gastrodin ameliorates anxiety-like behaviors and inhibits IL-1beta level and p38 MAPK phosphorylation of hippocampus in the rat model of posttraumatic stress disorder. *Physiol. Res.* 62 (5), 537–545. https://doi.org/10.33549/physiolres.932507.

Peres, T.V., Schettinger, M.R., Chen, P., Carvalho, F., Avila, D.S., Bowman, A.B., Aschner, M., 2016. Manganese-induced neurotoxicity: a review of its behavioral consequences and neuroprotective strategies. *BMC Pharmacol. Toxicol.* 17 (1), 57. https://doi.org/10.1186/s40360-016-0099-0.

Roh, E., Song, D.K., Kim, M.S., 2016. Emerging role of the brain in the homeostatic regulation of energy and glucose metabolism. *Exp. Mol. Med.* 48 (3), e216. https://doi.org/10.1038/emm.2016.4.

Roser, A.E., Tonges, L., Lingor, P., 2017. Modulation of microglial activity by rho-kinase (ROCK) inhibition as therapeutic strategy in Parkinson's disease and amyotrophic lateral sclerosis. *Front. Aging Neurosci.* 9, 94. https://doi.org/10.3389/fnagi.2017.00094.

Salar, S., Lapilover, E., Müller, J., Hollnagel, J.O., Lippmann, K., Friedman, A., Heinemann, U., 2016. Synaptic plasticity in area CA1 of rat hippocampal slices following intraventricular application of albumin. *Neurobiol. Dis.* 91, 155–165. https://doi.org/10.1016/j.nbd.2016.03.008.

Sarkar, S., Malovic, E., Harischandra, D.S., Ngwa, H.A., Ghosh, A., Hogan, C., Kanthasamy, A., 2018. Manganese exposure induces neuroinflammation by impairing mitochondrial dynamics in astrocytes. *Neurotoxicology* 64, 204–218. https://doi.org/10.1016/j.neuro.2017.05.009.

Schmidt, S.I., Blaabjerg, M., Freude, K., Meyer, M., 2022. RhoA signaling in neurodegenerative diseases. *Cells* 11 (9). https://doi.org/10.3390/cells11091520.

Sulzer, D., 2007. Multiple hit hypotheses for dopamine neuron loss in Parkinson's disease. *Trends Neurosci.* 30 (5), 244–250. https://doi.org/10.1016/j.tins.2007.03.009.

Takata, F., Nakagawa, S., Matsumoto, J., Dohgu, S., 2021. Blood-brain barrier dysfunction amplifies the development of neuroinflammation: understanding of cellular events in brain microvascular endothelial cells for prevention and treatment of BBB dysfunction. *Front. Cell. Neurosci.* 15, 661838. https://doi.org/10.3389/fncel.2021.661838.

Tao, J., Luo, Z.Y., Msangi, C.I., Shu, X.S., Wen, L., Liu, S.P., Hu, W.X., 2009. Relationships among genetic makeup, active ingredient content, and place of origin of the medicinal plant Gastrodia tuber. *Biochem. Genet.* 47 (1–2), 8–18. https://doi.org/10.1007/s10528-008-9201-7.

Tonges, L., Frank, T., Tatenhorst, L., Saal, K.A., Koch, J.C., Szego, E.M., Lingor, P., 2012. Inhibition of rho kinase enhances survival of dopaminergic neurons and attenuates axonal loss in a mouse model of Parkinson's disease. *Brain* 135 (Pt 11), 3355–3370. https://doi.org/10.1093/brain/aws254.

Vairappan, B., Sundhar, M., Srinivas, B.H., 2019. Resveratrol restores neuronal tight junction proteins through correction of ammonia and inflammation in CCl(4)-induced cirrhotic mice. *Mol. Neurobiol.* 56 (7), 4718–4729. https://doi.org/10.1007/s12035-018-1389-x.

Viellard, J., Baldo, M.V., Canteras, N.S., 2016. Testing conditions in shock-based contextual fear conditioning influence both the behavioral responses and the activation of circuits potentially involved in contextual avoidance. *Behav. Brain Res.* 315, 123–129. https://doi.org/10.1016/j.bbr.2016.08.033.

Wang, Q., Huang, X., Su, Y., Yin, G., Wang, S., Yu, B., Yi, C., 2022. Activation of Wnt/beta-catenin pathway mitigates blood-brain barrier dysfunction in Alzheimer's disease. *Brain* 145 (12), 4474–4488. https://doi.org/10.1093/brain/awac236.

Wang, D., Zhang, J., Jiang, W., Cao, Z., Zhao, F., Cai, T., Luo, W., 2017. The role of NLRP3-CASP1 in inflammasome-mediated neuroinflammation and autophagy dysfunction in manganese-induced, hippocampal-dependent impairment of learning and memory ability. *Autophagy* 13 (5), 914–927. https://doi.org/10.1080/15548627.2017.1293766.

Weissberg, I., Wood, L., Kamintsky, L., Vazquez, O., Milikovsky, D.Z., Alexander, A., Kaufer, D., 2015. Albumin induces excitatory synaptogenesis through astrocytic TGF-beta/ALK5 signaling in a model of acquired epilepsy following blood-brain barrier dysfunction. *Neurobiol. Dis.* 78, 115–125. https://doi.org/10.1016/j.nbd.2015.02.029.

Willis, C.L., Leach, L., Clarke, G.J., Nolan, C.C., Ray, D.E., 2004. Reversible disruption of tight junction complexes in the rat blood-brain barrier, following transitory focal astrocyte loss. *Glia* 48 (1), 1–13. https://doi.org/10.1002/glia.20049.

Wu, P., Kong, L., Li, J., 2019. MicroRNA-494-3p protects rat cardiomyocytes against septic shock via PTEN. *Exp. Ther. Med.* 17 (3), 1706–1716. https://doi.org/10.3892/etm.2018.7116.

Yang, R., Lv, Y., Miao, L., Zhang, H., Qu, X., Chen, J., Wang, X., 2021. Resveratrol attenuates meningitic Escherichia coli-mediated blood-brain barrier disruption. *ACS Infect. Dis.* 7 (4), 777–789. https://doi.org/10.1021/acsinfecdis.0c00564.

Zamboni, V., Jones, R., Umbach, A., Ammoni, A., Passafaro, M., Hirsch, E., Merlo, G.R., 2018. Rho GTPases in intellectual disability: from genetics to therapeutic opportunities. *Int. J. Mol. Sci.* 19 (6). https://doi.org/10.3390/ijms19061821.

Zhan, H.D., Zhou, H.Y., Sui, Y.P., Du, X.L., Wang, W.H., Dai, L., Jiang, T.L., 2016. The rhizome of Gastrodia elata Blume - An ethnopharmacological review. *J. Ethnopharmacol.* 189, 361–385. https://doi.org/10.1016/j.jep.2016.06.057.

Zhang, J.S., Zhou, S.F., Wang, Q., Guo, J.N., Liang, H.M., Deng, J.B., He, W.Y., 2016. Gastrodin suppresses BACE1 expression under oxidative stress condition via inhibition of the PKR/eIF2alpha pathway in Alzheimer's disease. *Neuroscience* 325, 1–9. https://doi.org/10.1016/j.neuroscience.2016.03.024.

Zhao, F., Cai, T., Liu, M., Zheng, G., Luo, W., Chen, J., 2009. Manganese induces dopaminergic neurodegeneration via microglial activation in a rat model of manganism. *Toxicol. Sci.* 107 (1), 156–164. https://doi.org/10.1093/toxsci/kfn213.

Zhao, Y., Gan, L., Ren, L., Lin, Y., Ma, C., Lin, X., 2022. Factors influencing the blood-brain barrier permeability. *Brain Res.* 1788, 147937. https://doi.org/10.1016/j.brainres.2022.147937.

Zlokovic, B.V., 2008. The blood-brain barrier in health and chronic neurodegenerative disorders. *Neuron* 57 (2), 178–201. https://doi.org/10.1016/j.neuron.2008.01.003.